

# Microstructural evaluation of thermally fatigued SiC-reinforced Al<sub>2</sub>O<sub>3</sub>/ZrO<sub>2</sub> matrix composites

S. H. KENAWY, W. M. N. NOUR

*Department of Refractories, Ceramics and Building Materials, National Research Centre, Dokki, Egypt*

*E-mail: ahmedsayed200@hotmail.com*

*E-mail: wagdynour@hotmail.com*

Using the water-quenching technique, the thermal fatigue behaviour of an alumina/zirconia and platelets- and particulates-SiC reinforced alumina/zirconia matrix composites hot-pressed at 1500 and 1700°C has been studied. The addition of 10 wt% SiC either in the form of platelets or particulates can obviously improve the thermal fatigue resistance of alumina/zirconia composites. The damages present after 40 thermal fatigue cycles in the composites was illustrated by the microstructure examinations and EDX.

© 2005 Springer Science + Business Media, Inc.

## 1. Introduction

The thermal fatigue resistance of ceramics is of particular importance in a variety of applications. Determination of this resistance is extremely important for their failure-free operation. To meet the needs of those applications, many different methods of characterizing the sensitivity of the ceramic material have been generated [1–6]. Methods for thermal fatigue resistance determination are divided into two basic groups: parameter methods and quenching methods.

Parameter methods are based on physical properties of the tested material (thermal expansion and heat conductivity, elastic modulus, Poisson's ratio, and mechanical strength) and thermal conditions prevailing in the given case of refractories services. From the theoretical point of view the parameter methods is the most rational but it is difficult and lengthy in execution, because the physical properties mentioned above change with temperature and at the same time thermal conditions of the given refractory service are seldom known sufficiently well.

On the contrary, quenching methods are finding widespread use in practice. They consist in heating up the sample to the specified temperature and determining the extent of the sample damage after a sudden cooling (quenching) in various media (air, water, liquid nitrogen, etc.). Normally several thermal cycles are required for achieving a measurable damage. The damage caused by thermal changes is determined using a number of methods, e.g. visually, by examining the microstructure, by weighing, by a measurements of change in ultrasound passage velocity, by measuring mechanical strength drop, etc.

When ceramic material is subjected to thermal fatigue, mechanical stress is generated therein. On exceeding the mechanical strength threshold, elastic strain

energy is released which is accompanied by the formation and propagation of cracks.

Silicon carbide in the form of whiskers has been most widely used as a reinforcing agent for Si<sub>3</sub>N<sub>4</sub> or oxide ceramics such as Al<sub>2</sub>O<sub>3</sub> or ZrO<sub>2</sub>. High strength, high modulus and chemical inertness at elevated temperatures made SiC the most suitable reinforcing agent. In many composites substantial improvements in fracture toughness and slow crack-growth resistance were obtained by reinforcement with SiC whiskers [7, 8]. It was considered that alumina/SiC nanocomposites have been researched intensively, they have significantly improved both bending strength and fracture toughness compared with the monolithic alumina. The aspects of the thermal shock resistance of sintered alumina/SiC nanocomposites was studied using indentation technique. It was found that addition of SiC nanophase as low as 1 vol% leads to surface damage thermal shock resistance superior to that of pure alumina [9]. When SiC-particles are added to alumina-zirconia matrix, the fracture toughness ( $K_{IC}$ ) is significantly improved compared to monolithic alumina or zirconia. For example, an alumina-zirconia-20 vol% SiC composite has a fracture toughness of  $K_{IC} = 12 \text{ Mpa/m}^2$  as compared to  $8.7 \text{ Mpa/m}^2$  [10]. Analysis of reinforcing mechanisms has indicated that crack deflection, crack bridging and pull out by platelets-SiC are the major toughening mechanisms with some contribution of crack propagation [11]. Because of their very attractive properties, the platelets- and particulate-SiC reinforced alumina-zirconia composites are good candidates for use in advanced heat engine, as cutting tools, and various other applications. An important consideration in many of those applications is the thermal fatigue resistance of the selected ternary system SiC-Al<sub>2</sub>O<sub>3</sub>-ZrO<sub>2</sub> ceramic materials.

TABLE I Characteristics of starting powders

	Alumina	3 mol% Y <sub>2</sub> O <sub>3</sub> - zirconia	$\alpha$ -SiC platelets	$\alpha$ -SiC particulates
Crystal structure	Corundum ( $\alpha$ -Al <sub>2</sub> O <sub>3</sub> ) hexagonal	Tetragonal and monoclinic ZrO <sub>2</sub>	Hexagonal polytypes	Hexagonal polytypes
Fired density (g/cm <sup>3</sup> )	3.97	5.99	3.22	3.18
Surface area (m <sup>2</sup> /g)	14.10	15.00	0.11	0.30
Purity (%)	99.90	99.90	99.90	99.90
Impurities content	Fe 6 ppm	Y <sub>2</sub> O <sub>3</sub> 5.090%	–	–
	SiO <sub>2</sub> 4 ppm	SiO <sub>2</sub> 0.009%		
	CaO 1 ppm	Na <sub>2</sub> O 0.018%		
	MgO 1 ppm	Al <sub>2</sub> O <sub>3</sub> < 0.005%		
	K <sub>2</sub> O 1 ppm	Fe <sub>2</sub> O <sub>3</sub> 0.002%		
		L.I.O 3.530%		

The main objective of the work in this paper is to evaluate the destructive action of cyclic thermal fatigue on the microstructure of platelets- and particulates-SiC reinforced Al<sub>2</sub>O<sub>3</sub>/ZrO<sub>2</sub> composites.

## 2. Experimental procedure

The materials used in this work were ultra-fine pure alumina and zirconia as well as two types of silicon carbide powders; namely, platelets and particulates. The alumina and zirconia were obtained from Boehringer Ingelheim Chemicals, and produced by Tosho, Japan, respectively, whereas platelets- and particulates-SiC were delivered from Millennium Materials, Matrix Enterprises Company, (MEC) USA, and Electroschmelzwerk Kempten GmbH, (ESK), respectively. Table I summarizes physical and chemical characterization of these materials.

Thermal fatigue experiment was conducted on the following hot-pressed composites: 90 wt% Al<sub>2</sub>O<sub>3</sub> + 10 wt% 3 mol% Y<sub>2</sub>O<sub>3</sub> stabilized ZrO<sub>2</sub> sintered at 1500°C (sample A<sub>9</sub>Z<sub>1</sub>) and 80 wt% Al<sub>2</sub>O<sub>3</sub> + 10 wt% 3 mol% Y<sub>2</sub>O<sub>3</sub> stabilized ZrO<sub>2</sub> + 10 wt% platelets- or particulates-SiC (samples A<sub>8</sub>Z<sub>1</sub>S<sub>1P</sub> or A<sub>8</sub>Z<sub>1</sub>S<sub>1Par</sub>, respectively) sintered at 1500 and 1700°C. The composite samples were prepared as mentioned in previous study [12]. The densification parameters of the tested samples are given in Table II.

Samples with the dimensions of 3 × 3.5 × 30 mm<sup>3</sup> were subjected to repeated thermal fatigue cycling at 1000°C. The thermal stability of the composite samples was measured by the water quench test (sever condition) as an experimental method. In each cycle the samples were held for 20 min at 1000°C in an electric furnace. The samples were then removed and quenched

in water for about 3 min before returning to the furnace at 1000°C. The procedure was repeated for 40 times.

The microstructure of the thermally fatigued samples was investigated using scanning electron microscope (SEM) model Philips XL 30 attached with EDX unit.

## 3. Results and discussion

In designing ceramic materials for application where thermal fatigue resistance is the major guiding factor two approaches are followed. The first of these uses in case of crucibles, turbine blades and other engine components, etc., aims at avoiding initiation of crack by thermal stress. However, when thermal environment is too severe to avoid fracture initiation, as in the case with furnace linings, combustor linings, etc., the second approach is resorted, which tries to minimize the extent of crack propagation. Incorporation of microstructural inhomogenities helps to arrest excessive crack propagation [13, 14]. A crack may be arrested when it reaches a pore. The role of porosity in enhancing the resistance to thermal fatigue damage is well known.

The A<sub>9</sub>Z<sub>1</sub> samples sintered at 1500 and 1700°C showed the lowest thermal fatigue resistance (5 cycles). This may be due to the difference of thermal mismatches between alumina ( $8.1-9.1 \times 10^{-6}/^{\circ}\text{C}$ ) and tetragonal zirconia ( $11.6 \times 10^{-6}/^{\circ}\text{C}$ ). In composite materials, the difference in thermal expansion coefficient of the components is responsible for generating the microcracks [15]. In fact, the phase inversions of zirconia during thermal cycling offer an effective stress relief mechanism. During the heating cycle, the transformation of the monoclinic phase to the tetragonal phase is accompanied by an appreciable reduction in volume while the bulk material is expanding. During the cooling cycle, the tetragonal form reverts to the monoclinic form without consequent increase in volume in a contacting body. These volume changes during thermal cycling introduce extensive microcracks, which propagate through the whole body [16]. The incorporation of 10 wt% of either platelets- or particulates-SiC to A<sub>9</sub>Z<sub>1</sub> sample, on the expense of alumina, rises its thermal fatigue resistivity from 5 to more than 40 cycles. The low coefficient of thermal expansion coupled with a high thermal conductivity of SiC contributes to the high thermal fatigue-resistance of samples A<sub>8</sub>Z<sub>1</sub>S<sub>1P</sub> and A<sub>8</sub>Z<sub>1</sub>S<sub>1par</sub>.

TABLE II Densification parameters of the tested composites

Sample	Sintering temperature			
	1500°C		1700°C	
	*B.D (g/cm <sup>3</sup> )	A.P (%)	B.D (g/cm <sup>3</sup> )	*A.P (%)
A <sub>9</sub> Z <sub>1</sub>	4.17	0.00	4.04	0.46
A <sub>8</sub> Z <sub>1</sub> S <sub>1P</sub>	4.06	0.36	4.07	0.61
A <sub>8</sub> Z <sub>1</sub> S <sub>1Par</sub>	4.09	0.76	4.04	0.95

\*B.D = Bulk density.

\*A.P = Apparent porosity.

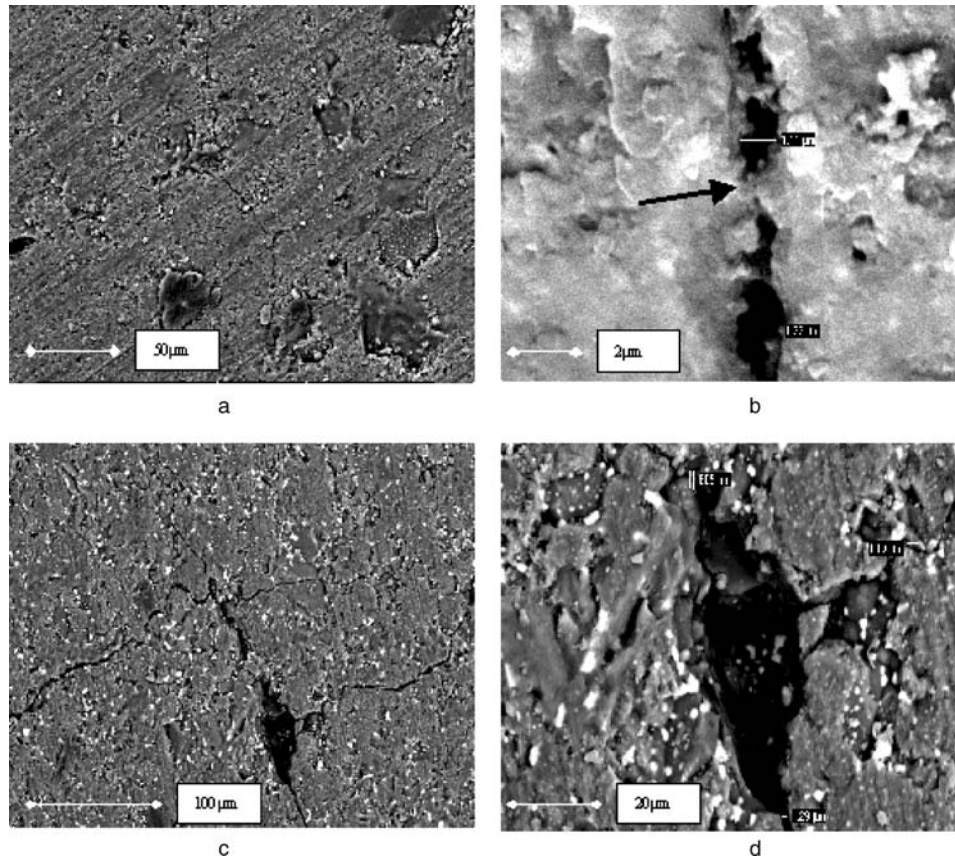


Figure 1 Scanning electron micrographs of thermally fatigued  $A_8Z_1S_{1p}$  sample: (a, b) sintered at 1500°C and (c, d) sintered at 1700°C.

SEM micrographs of the  $A_8Z_1S_{1p}$  and  $A_8Z_1S_{1par}$  samples after 40 thermal fatigue cycles are shown in Figs 1 and 2, respectively. Table III shows the statistics of approximate crack density of the thermally fatigued samples. Figs 1a and b show the microstructure of thermally fatigued  $A_8Z_1S_{1p}$  hot-pressed at 1500°C. It can be seen that a massive cracking is observed which propagate through the whole sample (Fig. 1a). Cracks occasionally branched out from the main cracks. It was reported [17] that residual thermal stresses, in platelets-SiC reinforced  $Al_2O_3/Y-TZP$  composites, are created at the platelets/matrix interface during cooling from the sintering temperature due to thermal mismatch between the SiC platelets ( $\alpha = 4 \times 10^{-6}/^\circ C$ ), and phases of the matrix:  $Al_2O_3$  ( $\alpha = 8 \times 10^{-6}/^\circ C$ ) and yttria stabilized tetragonal zirconia polycrystals (Y-TZP) ( $\alpha = 10 \times 10^{-6}/^\circ C$ ). Since  $\alpha_{matrix} > \alpha_{platelets}$ , it is expected that the SiC platelets are subjected to compressive stress and  $Al_2O_3/Y-TZP$  matrix to tangential tensile stresses, resulting in radial microcracks around the platelets. The appearance of a plate-like morphology over the surface of the sample is possibly as a consequence of the re-

moval of the carbon interface allied with oxidation of the SiC. Since the specific volume of silica is almost twice that of carbon then the silica is likely to exude out of the interface and over the surface. Fig. 1b reveals that the crack is opened forming a very large pores with a diameter ranged from 1.11 to 1.33  $\mu m$ . A crack bridging by viscous glassy phases was observed (marked by an arrow). These glassy phases may be due to the oxidation of SiC into  $SiO_2$ , which in turn reacts with the surroundings  $Al_2O_3$  forming aluminosilicate glassy phases.

Figs 1c and d show a typical morphology of thermally fatigued  $A_8Z_1S_{1p}$  sample hot-pressed at 1700°C observed with SEM. It is clear that the cracks propagated through the whole sample (Fig. 1c). The width of these cracks and the volume of the bright phase ( $ZrO_2$  particles) are increased as compared with the same thermally fatigued sample hot-pressed at 1500°C. This increment in volume of  $ZrO_2$  particles may be attributed to its transformation. A very large cavity like void with a rounded edge is shown in Fig. 1d. The thermal mismatches between alumina and zirconia aggravated the stress and caused a rounded contour formation. The pores served as sink for absorption of stress and strain. It was shown earlier [18] that pore size increased with the progress of thermal-fatigue cycling and pseudoplasticity developed in  $Al_2O_3/ZrO_2$  composite.

Figs 2a–c show the microstructure of the thermally fatigued  $A_8Z_1S_{1par}$  sample hot-pressed at 1500°C. Fig. 2a reveals a microcracks with different widths ranged from 298–547 nm through the whole sample. The variations in crack length and width after thermal

TABLE III Statistics of approximate crack density

Sample type	Area ( $mm^2$ )	Crack no.	Crack length ( $\mu m$ )	Crack opening ( $\mu m$ )
$A_8Z_1S_{1p}$ (1500°C)	49.45	9	13	1.11–1.33
$A_8Z_1S_{1p}$ (1700°C)	119	7	100–250	0.806–35
$A_8Z_1S_{1par}$ (1500°C)	119	3	10–25	0.298–0.547
$A_8Z_1S_{1par}$ (1.7500°C)	19.32	5	40–80	109

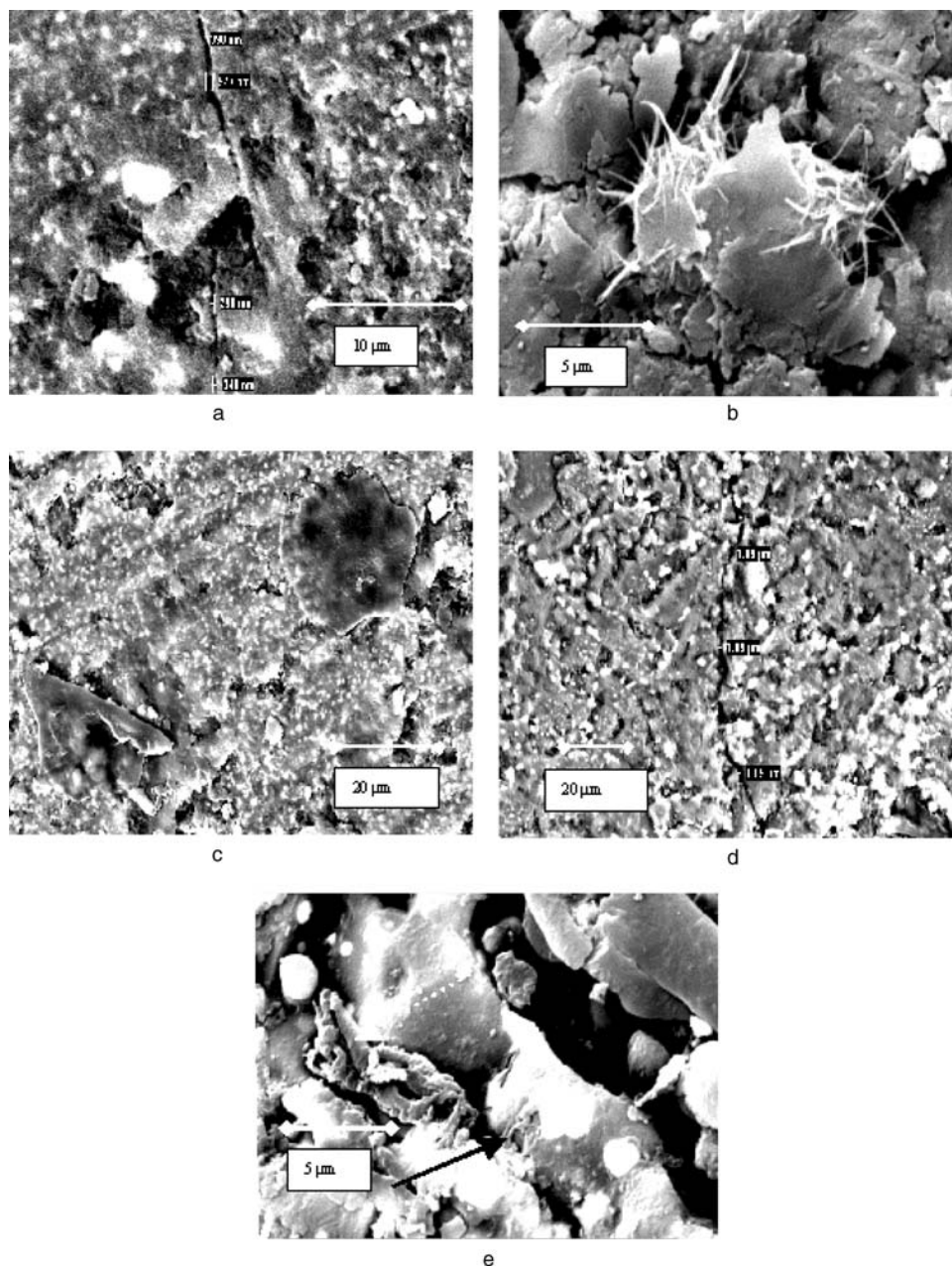


Figure 2 Scanning electron micrographs of thermally fatigued  $A_8Z_1S_{1par}$  sample: (a, b, c) sintered at  $1500^\circ\text{C}$  and (d, e) sintered at  $1700^\circ\text{C}$ .

cycling was attributed to the initiations of cracks in the regions of tensile stress (cold regions) and propagate into the regions of compressive stress (hot region) [19].

Viscous glassy phases in the form of a fibrous aluminosilicate are seen (Fig. 2b). The spectra of EDX-point analysis confirmed that the chemical composition of the fibrous structure is an  $Al_2O_3$ -rich aluminosilicate (Fig. 3a). Also, the generated  $SiO_2$  tends to form a plate-like morphology over the whole surface (Fig. 2c). It was concluded [20–22] that an aluminosilicate glassy phases (54–66%  $Al_2O_3$  and 33–45%  $SiO_2$ ) are formed at the grain boundaries of alumina grain in contacts with SiC particles. The composition, crystallinity and amount of these glassy phases depend on the time and temperature of oxidation [23]. It was suggested [24] that the incorporation or in situ formation of lower melting point glassy phases into the refractory ceramics could improve the body life. Such phases can promote additional improvements in the ceramic body

life by extending the temperature regime for strain accommodation/relaxation by viscous flow and possible crack-bridging and/or crack-sealing phenomena down to lower-temperature.

The microstructure of  $A_8Z_1S_{1par}$  sample hot-pressed at  $1700^\circ\text{C}$  is illustrated in Fig. 2d and e. It is clear that a thin, dense and vitreous layer of glassy phases is significant and adjacent to the SiC particles, this glassy phase was flowed uniformly all over the sample Fig. 2d. If Fig. 2a and d are compared, it can be seen that sintering of  $A_8Z_1S_{1par}$  sample at  $1700^\circ\text{C}$  results in more damage as it is obvious from crack width measurement. This may be attributed to more zirconia transformation upon sintering at  $1700^\circ\text{C}$ . As shown in Fig. 2e, the zirconia particles undergoes a martenistic tetragonal to monoclinic phase transformation (as marked by a solid arrow). This transformation is accompanied by volume increase, followed by twining of particles. It was reported [25] that the transformation from *t*- to *m*- $ZrO_2$

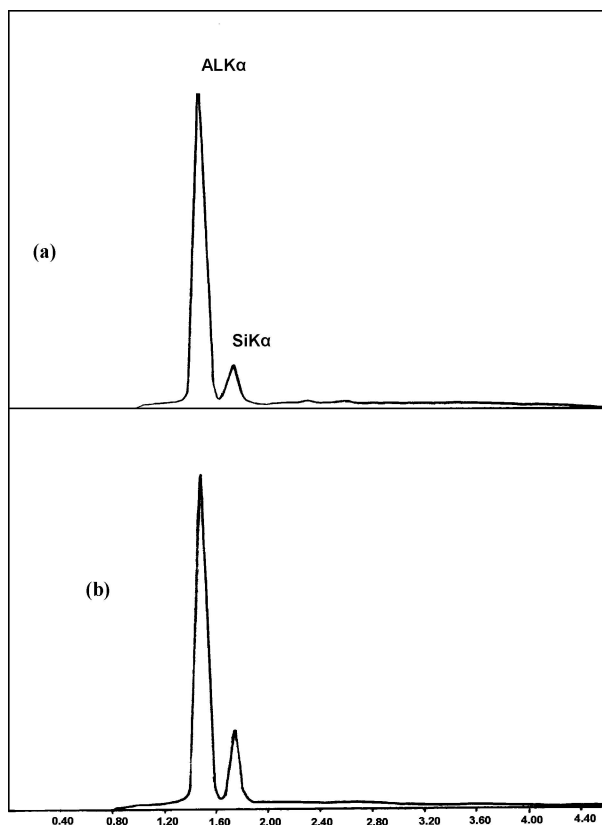


Figure 3 Energy dispersive X-ray analysis of (a) fibrous structure (Fig. 2b) and thread-like structure (Fig. 2e).

on cooling shows a high volume expansion of 3–5%. A thread-like structure (as marked by a dashed arrow in Fig. 2e) is observed of an  $\text{Al}_2\text{O}_3$ -rich aluminosilicate composition as was analyzed by EDX (Fig. 3b).

#### 4. Conclusion

This work has studied the effect of introducing 10 wt% SiC on the ability of  $\text{Al}_2\text{O}_3/\text{ZrO}_2$  composite to resist thermal fatigue cycling through examining their microstructure. The investigated composites showed that the increase in the lifetime of 5 thermal cycles for  $\text{A}_9\text{Z}_1$  composite to more than 40 thermal cycles for  $\text{A}_8\text{Z}_1\text{S}_{1\text{p}}$  and  $\text{A}_8\text{Z}_1\text{S}_{1\text{par}}$  composites is mainly due to the incorporation of SiC either in the form of platelets or particulates and the presence of glassy phases as detected by EDX. The glassy phases can have at least two potential beneficial effects. First, The phases are likely to accommodate or relax thermal/residual stress during up quenching or down quenching. Second, the vis-

cous glassy phases can be used to promote crack tip shielding by bridging cracks under thermal cycling conditions. Thermal mismatches and zirconia inversions in the tested composites under thermal cycling lead to microcracking.

#### References

1. J. RANACHOWSKI, F. REJMUND and Z. LIBRANT, Akustyka w badaniach materialow ceramicznych. Institute of Basic Problems Technology, Report IPPT. 28/1984
2. M. BONIECKI and Z. LIBRANT, Analiza wlasnosci mechanicznych materialow ceramicznych metodami mechaniki pekania. Institute of Electronic Materials Technology, Reports ITM 14/1984.
3. J. RANACHOWSKI, F. REJMUND and Z. LIBRANT, *Archiwum Nauki o Materialach* **6** (1985) 211.
4. J. RANACHOWSKI, F. REJMUND and M. BONIECKI, *Engng. Trans.* **32** (1984) 329.
5. I. ELSTNER and P. JESCHE, *Sprechaal* **111** (1982) 288.
6. G. C. ROBINSON, C. R. REESE and E. A. JR. LAROCHE, *Amer. Ceram. Soc. Bull.* **53** (1974) 482.
7. H. KODAMA, J. SUZUKI, H. SAKAMOTO and H. MIYOSHI, *J. Amer. Ceram. Soc.* **73** (1990) 678.
8. G. PEZZOTTI, *ibid.* **76** (1993) 1313.
9. S. MAENSIRI and S. G. ROBERTS, *J. Euro. Ceram. Soc.* **22** (2002) 2945.
10. HYUN M. JANG, H. MOOM and CHEOL W. JANG, *J. Amer. Ceram. Soc.* **75** (1992) 3369.
11. T. N. TIEGS and P. F. BECHER, *ibid.* **70** (1987) C-109.
12. S. H. KENAWY, PhD Thesis, Fakultät für Bergbau, Hütten Wesen und Geowissenschaften der Rheinisch- der Westfälischen Technischen Hochschule Aachen, Aachen, 2000.
13. D. P. H. HASSELMAN, *J. Amer. Ceram. Soc.* **46** (1963) 535.
14. *Idem.*, *ibid.* **52** (1969) 600.
15. N. C. BISWAS and S. P. CHAUDHURI, *Ceram. Intern.* **23** (1997) 69.
16. D. P. H. HASSELMAN, in "Mat. Sci. Res.- Ceramics in Severe Environment," edited by W. W. Kriegel and H. P. Palmour (Plenum Press, New York, 1971) p. 89.
17. C. KAYA, F. KAYA, P. A. TRUSTY, A. R. BOCCACCINI and M. MARSOGLU, *Ceram. Intern.* **25** (1999) 359.
18. B. L. MITRA, N. C. BISWAS and P. S. AGGARWAL, *Bull. Mater. Sci.* **15** (1992) 131.
19. T. J. LU and N. A. FLECK, *Actam. Mater.* **46** (1998) 4744.
20. LINUS U. J. T. OGBJI, *Ceram. Intern.* **12** (1986) 173.
21. CHENG-YUAN TSAI and CHIEN-CHENG LIN, *J. Amer. Ceram. Soc.* **81** (1998) 2413.
22. C. H. R. KÖPP, K. MITTAG and H. HAUSNER, *Cfi/Ber. DKG* **73** (1996).
23. P. WANG, G. GRATHWOHL, F. PROZ and F. THÜMLER, *Powder Metall. Intern.* **23** (1991).
24. JOACHIM H. SCHNEIBEL, STEPHEN M. SABOL, MAY MORRISON, EVAN LUDEMAN and CECIL A. CARMICHAEL, *J. Amer. Ceram. Soc.* **83** (1998) 1888.
25. F. F. LANGE, *J. Mat. Sci.* **17** (1982) 225.

Received 5 May 2003

and accepted 25 August 2004